# HIGH THROUGHPUT SURFACE STRUCTURING WITH ULTRASHORT PULSES IN SYNCHRONIZED MODE WITH FAST POLYGON LINE SCANNER

Paper M203

Beat Neuenschwander[1], Beat Jäggi[1], Markus Zimmermann[2], Lars Penning[3], Ronny de Loor[3], Kurt Weingarten[4] and Andreas Oehler[4]

[1] Bern University of Applied Science, Institute for Applied Laser, Photonics and Surface Technologies, Pestalozzistrasse 20, 3400 Burgdorf, Switzerland
[2] Bern University of Applied Science, Institute for Mechatronic Systems, Pestalozzistrasse 20, 3400 Burgdorf, Switzerland
[3] Next Scan Technology, Ulftseweg 14, BD Silvolde, 7064, The Netherlands
[4] Time-Bandwidth Products AG, Ruetistrasse 12, 8952 Schlieren, Switzerland



## Abstract

High precision laser micromachining requires an exact synchronization of the laser pulse train with the mechanical axes of the motion system to ensure for each single pulse a precise control of the laser spot position - on the target. For ultra short pulsed laser systems this was already demonstrated with a conventional two-axis galvanometer scanner. But this solution is limited by the scanner architecture to a marking speed of about 10m/s with a maximum scan line length of about 100mm. It is therefore not suited for average powers far beyond 10W when working at the optimum point with highest removal rate and machining quality is desired. A way to overcome this limitation is offered by polygon line scanners which are able to realize much higher lateral speeds at large scan line lengths.

In this work we will report on the results with a polygon line scanner having a maximum moving spot velocity of 100m/s, a scan line length of 170mm, spot diameters of 45µm (1064nm) and 22µm (532nm) together with a 50W, 10-ps laser system. The precise control of the laser spot position i.e. the synchronization is realized via the new SuperSync™ technology. Decoating, perforation and 3D patterning will act as benchmark processes to evaluate this scanning technology.

## Introduction

### Synchronized Marking

The standard process for surface structuring applications is the filling of a given outline with a parallel hatching. The lines of the hatch pattern are usually generated with galvo-scanners, and the laser pulse train is switched on and off via an external modulator which is gated by a signal from the scanner control software. Fig. 1 shows the different situations that can appear at the border of a structure. If the pulse train is switched on with the start of the axes acceleration, the distance from pulse to pulse (pitch) increases until the axes has reached its final speed (fig. 1a). Such lines show deep marks at the start and ending points of the single lines but the effective position of these points are well defined. To avoid this phenomenon of deep marking a so called sky-writing option can be used. Sky-writing means that the axes already have the correct velocity at the beginning of the marking. With this option a displacement of the start position of plus/minus half the distance between two consecutive pulses has to be accepted (fig. 1b) leading to inaccuracies due to the asynchronous motion of the axes relative to the pulse train. If this problem should be avoided it will be necessary to synchronize the axes motion onto the output pulse train of the laser system or vice versa (fig. 1c).

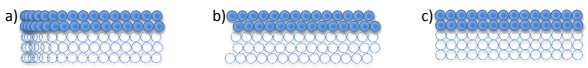


Fig. 1: Start positions of the different strategies: a) standard setup without sky-writing option; b) standard setup with the sky-writing option; c) synchronized system.

With this kind of synchronization the structuring information cannot longer be given in a vector format as typically used for galvo-scanners. A very simple way is the representation in a bitmap format where every pixel denotes a laser pulse as illustrated in fig. 2. White pixels mean laser off and black pixels laser on or vice versa. Additionally the coordinates of the starting point $(x_0, y_0)$, e.g. the upper left corner, have to be given and the pitches (distance from pulse to pulse) $p_x$ and $p_y$ have to be defined. It is clearly noted here that in contrast to

fig. 2 the pitches are often smaller than a spot diameter and that they can differ in $x$- and $y$-direction.

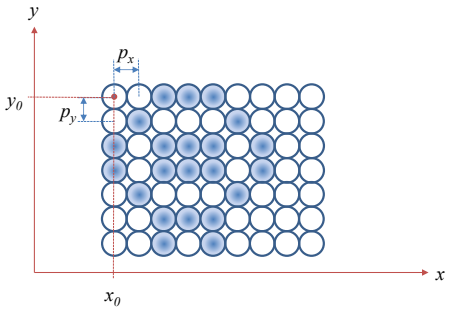


Fig. 2: Representation of the structuring information in a bitmap format where every pixel represents a potential laser pulse. Here white pixels mean laser off and "blue" pixels laser on. Here the upper left corner is defined as starting point with the coordinates $x_0$ and $y_0$ and the pitches in $x$- and $y$-direction are $p_x$ and $p_y$, respectively.

This kind of synchronization was realized with a conventional galvo-scanner [1,2] or on a rotating cylinder [3] and led to the following findings:

- Best surface roughness was obtained with a pitch of half a spot radius $w_0$ i.e. with $p_x = p_y = p = w_0/2$.
- To avoid regular patterns at the bottom of a structure the starting point ($x_0$, $y_0$) has to be slightly shifted in both directions from slice to slice. Best results were obtained with a random normal distribution for these shifts with a standard deviation of $p/4$ and of course a mean value of $x_0$ or $y_0$.
- Minimum achievable structure dimensions are in the range of a spot radius $w_0$.
- The steepness of wall i.e. the taper angle in the synchronized mode equals the situation with the acceleration problem (fig. 1a) and is much better than in the sky-writing mode, as illustrated in fig.3.

It is noted here the arbitrary shift of the starting point ($x_0$, $y_0$) will lead to slightly fuzzy borders but its extension of about $\pm w_0/8$ and is about one magnitude smaller than that of the sky-writing strategy with an uncertainty of $\pm w_0$.

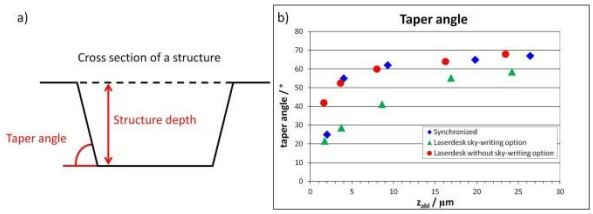


Fig. 3: a) Cross section of a structure; b) the taper angle versus the structure depth on the right side.

## Ablation Efficiency

For high precision micro machining the material parameters are important. As a consequence of the two-temperature-model which is discussed in the literature [4-6], the ablation depth $z_{abl}$ logarithmically depends on the applied fluence $F$:

$$z_{abl} = \delta \cdot \ln\left(\frac{F}{F_{th}}\right) \qquad (1)$$

with the two material parameters penetration depth $\delta$ and threshold fluence $F_{th}$. The threshold fluence $F_{th}$ describes the minimum energy which is needed to ablate material. The penetration depth $\delta$ is the ability of the energy to penetrate into the material. Due to this nonlinear ablation law the removal rate in ablated volume per time and average power strongly depends on the applied fluence and reads for a Gaussian beam following [7-10]:

$$\frac{\dot{V}}{P_{av}} = \frac{1}{4} \cdot \frac{\delta}{F} \cdot \ln^2\left(\frac{2 \cdot F}{F_{th}}\right) \text{ with: } F = \frac{E_p}{w_0^2 \cdot \pi} \qquad (2)$$

This removal rate shows a maximum value at an optimum fluence $F_{opt}$ given by:

$$\frac{\dot{V}_{\max}}{P_{av}} = \frac{\delta}{F_{opt}} \quad \text{and} \quad F_{opt} = \frac{e^2}{2} \cdot F_{th} \qquad (3)$$

Both measures depend on the material parameters $F_{th}$ and $\delta$.

## Consequences and requirements

The value for the optimum fluence $F_{opt}$ going with the highest removal rate (3) is only about 3.7 times higher than the threshold fluence $F_{th}$ i.e. its value is quite small. For copper and steel 1.4301 the threshold fluences amount about 0.3 $J/cm^2$ and 0.055 $J/cm^2$ [11] for 10 $ps$ pulses at a wavelength of 1064 $nm$, going with optimum fluences of about 1.1 $J/cm^2$ and 0.2 $J/cm^2$. For a spot

with 20 µm radius this corresponds to pulse energies of 14 $\mu J$ and and 2.5 $\mu J$ for copper and steel, respectively. For copper and an average power of 10 $W$ this would correspond to a repetition rate of about 700 kHz and a marking speed of more than 7 m/s when the pitch should amount half a spot radius. For steel these values amount to about 4 $MHz$ and 40 $m/s$ which is already above the capabilities offered by galvo scanners. The situation becomes more severe for an average power of 50 W where all these values multiply by 5. To work with galvo scanners and high average powers one has therefore either to reduce the pitch and taking heat accumulation effects and quality reductions into account or one uses -higher fluences resulting in a lower removal rate and also reduced quality. To still take benefit of the optimum fluence with maximum removal rate and quality one has therefore to use alternative concepts. One possibility is to parallelize the machining process e.g. with diffractive optical elements [12] has another alternative is to use faster scanning systems. One possibility to reach higher marking speeds is the combination of a fast rotating cylinder with fast deflector axes e.g. AOD's as presented in [13,14]. Another possibility is offered by polygon scanners [15,16] where the laser beam is guided via a fast rotating polygon mirror wheel and a flat field focusing optics onto the work piece resulting in a fast, unidirectional linear motion of the laser spot as illustrated in fig. 4. For a 2D marking, an additional motion perpendicular to the marking direction is necessary and the pattern is then generated in a raster scan process by switching single pulses on and off. To guarantee highest possible accuracy at a pitch in the range of the spot radius the polygon scanner has to be synchronized with the laser system which is a challenging task with a mode-locked laser system.

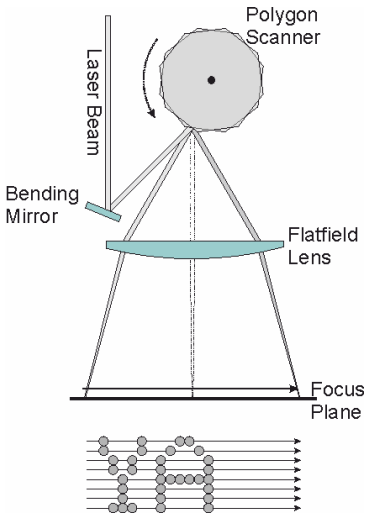


Fig. 4: Working principle of a polygon line scanner.

## Experimental Set-Up

An LS170A line scan engine from NextScan Technology is used as polygon scanner together with a FUEGO ps-laser system from Time-Bandwidth products. The line scanner has a polygon-wheel with 8 facets, a marking line length of 170 $mm$, marking speeds ranging from 25 $m/s$ – 100 $m/s$ and marking of 100 to 400 lines per second resulting in a duty cycle of about 70%. In contrast to most scanning systems here the focusing optic is set up with dichroic coated mirrors for the wavelengths 1064 $nm$ and 532 $nm$. The focal length of this objective amounts to $f$=190 $mm$ resulting in $1/e^2$ focus diameters of 45 $\mu m$ for 1064 $nm$ and 22 $\mu m$ for 532 $nm$ with a 6 $mm$ entrance beam diameter. The motion perpendicular to the scan direction is realized with a linear stage from Jenny Science which was slaved to LSE170 controller quadrature encoder output. An additional shorter linear stage in scan-direction is used for the random normal distributed shift of the starting point as described above. The whole set-up is shown in fig. 5. Black and white bitmaps served as input for the LSE170 controller. The FUEGO laser system emits 10 ps laser pulses at 1064 nm, 532 nm and 355 nm (not used in the presented experiments) with a beam quality $M^2 < 1.1$. The repetition rate can be varied from single pulses up to 8 MHz with a Pulse on Demand (PoD) option working up to 3 $MHz$ which is to the best of our knowledge the highest available frequency on the market for an industrial PoD. The average power at the repetition rate of 2 $MHz$ amounted to 42 $W$ for 1064 $nm$ and 15.3 $W$ for 532 $nm$ in front of the line scanner. The precise control of the laser spot position at the start of each line i.e. the synchronization is realized via the new SuperSync™ technology. All presented experiments were done with a laser repetition rate of 2 MHz. As marking speeds 25 $m/s$, 50 $m/s$, 70 $m/s$ and 95 $m/s$ resulting in pitches in scan direction of 12.5 $\mu m$, 25 $\mu m$, 37 $\mu m$ and 47.5 $\mu m$ were used.

Marking of isolated pulses with different bitmaps, dicing as well as 2D and 3D patterning have acted as processes to characterize and evaluate this scanning technology.

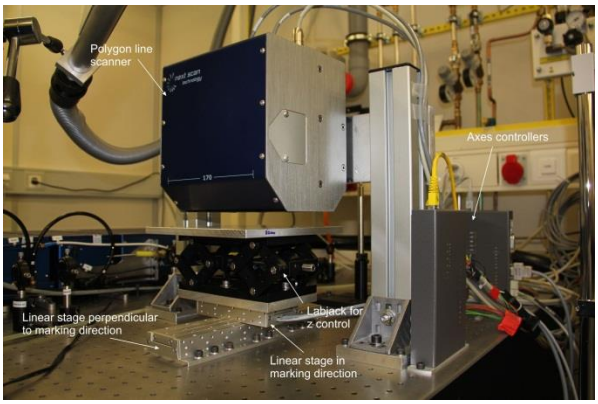


Fig. 5: Laboratory set up with polygon scanner and linear axes.

## Experimental Results

### Position accuracy

In a first experiment 50 lines with 4832 pixel per line were marked on glass plates with a 100 *nm* chromium coating with a wavelength of 532 *nm* and a marking speed of 70 *m*/*s* resulting in a pitch of 37 $\mu m$ at the repetition rate of 2 *MHz*. The average power amounted to 15.3 *W* in front of the scanner and the pitch perpendicular to the scan direction also amounted to 37 $\mu m$. Due to the smaller spot diameter of about 22 $\mu m$ the single shots were completely separated and could be analysed under an optical microscope as shown in fig. 6.

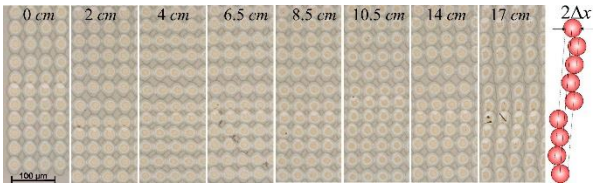


Fig. 6: Details of the spot pattern at different distances measured from the start position of the marked lines. On the right the principle for the derivation of the deviation from the central position is shown.

It can clearly be seen that the starting positions of the single marked lines are really synchronized. With increasing distance to the starting position the deviation of the spot positions of the expected central position increases but rests within the specified accuracy of $\pm 5$ $\mu m$. As a consequence of the uncorrected pyramidal error [17] (discussed later) the distance between the single lines varies as it can easily be seen.

For further investigations of the position accuracy similar experiments were performed with 1064 nm at the four different marking speeds 25 *m*/*s*, 50 *m*/*s*, 70 *m*/*s* and 95 *m*/*s*. To achieve a pulse separation of about 100 $\mu m$ in marking direction only every 8th, 4th, 3rd and 2nd pixel was marked. Marking eight lines one below the other shows the behaviour of all eight facets of the polygon wheel whereas adding seven blank lines after each marked line demonstrates the behaviour of only one single facet. For the latter the line pitch i.e. the speed of the linear axes has to be adapted to achieve the same line distance. An overview at the line start, in the middle end at the end of the 17 cm long line is shown in fig. 7. The deviations of the central positions were measured corresponding to fig. 6 and its results are summarized in fig. 8. Quite high deviations up to 35 $\mu m$ for 8 facets and 15 $\mu m$ for one single facet are observed for the lowest marking speed of 25 *m*/*s*. The deviations decrease for higher marking speeds and are always higher for 8 facets than for a single facet. The specified accuracy of $\pm 5$ $\mu m$ is not always reached.

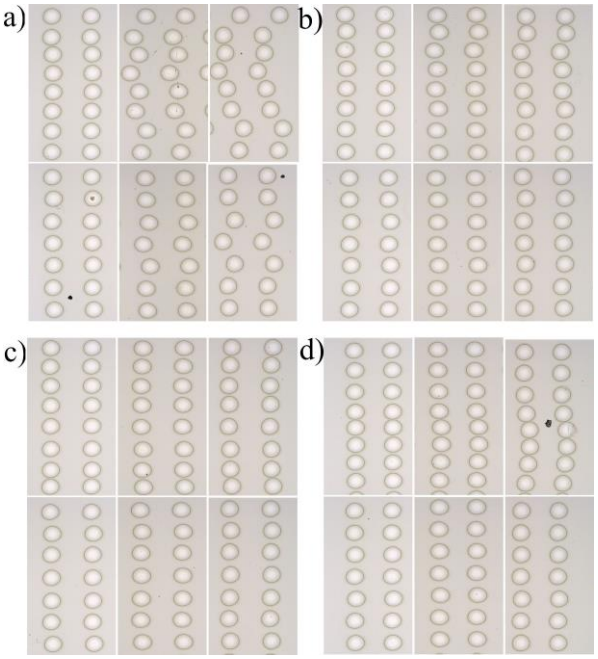


Fig. 7: Spot pattern for a) 25 *m*/*s*, b) 50 *m*/*s*, c) 70 *m*/*s* and d) 95 *m*/*s* marking speed at the start (left), in the middle (center) and the end (right) of the marking line. The upper row always shows the results for 8 facets and the lower row for one single facet. The horizontal distance between two spots amounts to exactly 100 $\mu m$ for 24 *m*/*s* and 50 *m*/*s*.

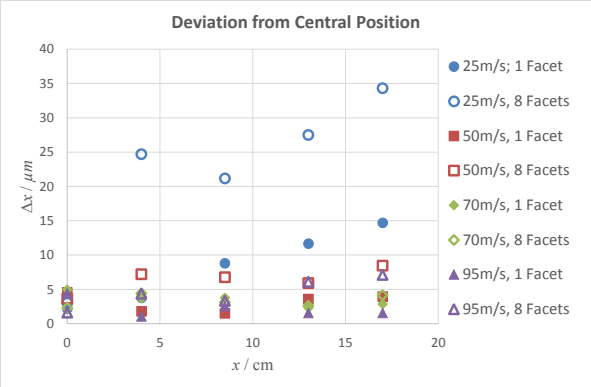


Fig. 8: Deviation from the central position as a function of the distance to the line start for 8 facets and one single facet and marking speeds of 25 *m/s*, 50 *m/s*, 70 *m/s* and 95 *m/s*.

To compare the 8 single facets a group of 11 lines with seven blank lines between each was followed by 14 blank lines resulting in a jump of one facet from group to group. For these experiments the coated glass was replaced by a black coated paper. The corresponding results for all marking speeds are presented in fig. 9 where the start and the end of the marking lines are presented for each of the 8 groups of eleven lines i.e. for each of the 8 facets.

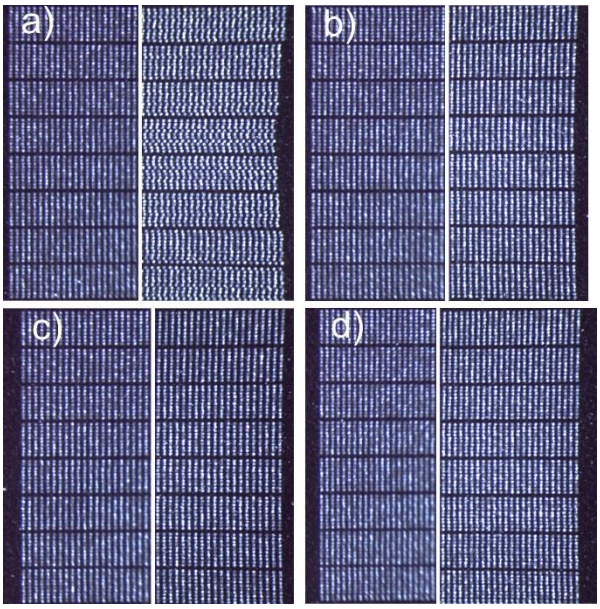


Fig. 9: Groups of 11 horizontal lines written with one single facet for the marking speeds a) 25*m/s*, b) 50*m/s*, c) 70*m/s* and d) 95*m/s*. From top down the facet is changed from group to group.

Again the line start position is fully synchronized for all marking speeds and facets but for the low marking speeds the spot positions at the line end again varies and also a variation of this position between the single facets can be observed. Also this deviation decreases with increasing marking speed. Another effect is observed at the start of the marking lines when the speed is changed. With increasing speed the start of the marked line is shifted into the scan direction as illustrated in fig. 10 for the steps from 25 to 50*m/s*, from 50 to 70*m/s* and from 70 to 95*m/s*. For the two 25*m/s* steps the shift amounted to about 550 $\mu m$ and for the 20*m/s* step it was about 470 $\mu m$. The reason for this shift is not known at the moment and it as only to be taken into account if the absolute position of the spots on the work piece becomes essential.

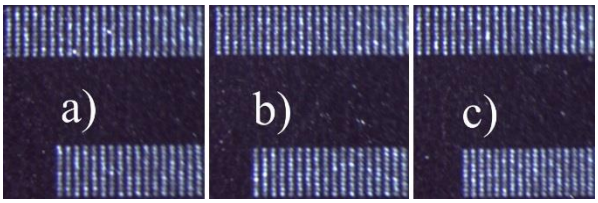


Fig. 10: Shift of the marked line into the scan direction when the marking speed is increased a) from 25 to 50*m/s*, b) from 50 to 70*m/s* and c) from 70 to 95*m/s*.

## Repeatability

To deduce the repeatability three lines were marked 2, 4, 8 and 16 times with a marking speed of 70 *m/s*, a repetition rate of 2 *MHz* and with 532 *nm* wavelength on a silicon wafer. Due to the small spot sizes at the green wavelength the pulses were automatically separated. A strongly increasing spot size would indicate a bad repeat accuracy but one has to also take into account the incubuation effect. The incubation leads to a decreasing threshold fluence with increasing pulse number [7,18] also resulting in an increasing spot size. This effect is more pronounced for low pulse numbers as used here. To distinguish between the spot size increase by repeatability and incubation also spots with stopped polygon wheel and the same number of pulses were marked. For both situations the spot size was determined by measuring the area of the marked spots and calculating a corresponding radius as illustrated in fig. 11.

The deduced spot radii for the stopped polygon and the scan lines as a function of the pulse number are shown in fig. 12. The maximum difference is 300 *nm* which is below the measurement uncertainty. From these experiments one can assume that the repeatability at a marking speed of 70 *m/s* is in the range of $\pm 1$ $\mu m$.

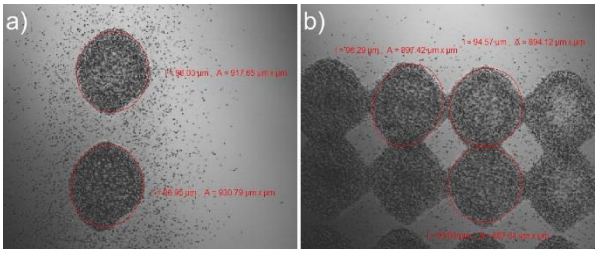


Fig. 11: Deduction of the spot area for 8 pulses with a) stopped polygon an b) marked scan line.

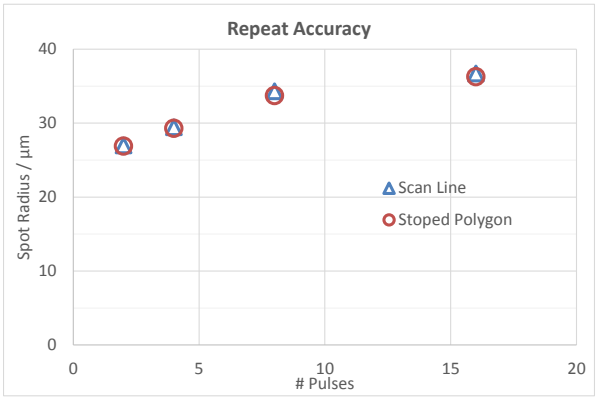


Fig. 12: Calculated spot radius for the spots in the scan line and with the stoped polygon as a function of the pulse number.

## Wafer Dicing

Wafer dicing was tested with a 50 $\mu m$ thin 6 inch silicon wafer. The laser worked at its maximum power of 43 $W$ in front of the scanner at a repetition rate of 2 *MHz* and the marking speed was 25 *m*/*s*. The wafer was cut after about 1000 lines i.e. 10 *s* for 170 *mm* cut length, but as shown in fig. 13 the surrounding of the cut is covered by debris. Further investigations with higher repetition rate and marking speeds up to 8 *MHz* at 100 *m*/*s* are needed to test if the debris could be reduced and the cutting speed increased.

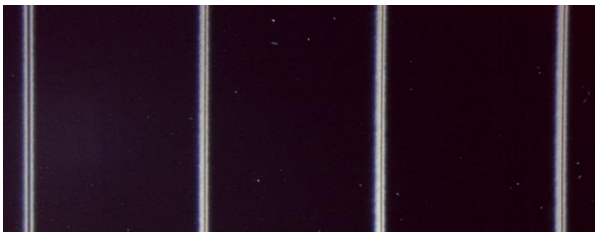

Fig. 13: Cuts in 6 inch silicon wafer.

## 2D structuring

To test 2D structuring greyscale bitmaps of Marylin Monroe [19] were converted with a Floyd-Steinberg algorithm to black and white bitmaps. A first series with 10.6 *mm* side length was marked twenty times on stainless steel 1.4301 with the wavelength of 532 *nm*, a marking speed of 70 *m*/*s*, an average power of 15.3 *W* and a repetition rate of 2 *MHz*. Fig. 14 show the 2x2 marked pictures at the left side a) and the right side b) of the marking area. When the colour difference between these two pictures is deduced it rests almost totally black and is therefore not shown here. This result means that the two pictures only show minimum deviations i.e. that there is almost no difference over the 17 *cm* long marking area. The periodic structure perpendicular to the marking direction is caused by the uncorrected pyramidal error.

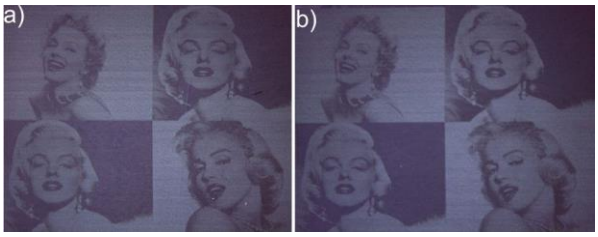


Fig. 14: 2x2 marked picture on the a) left side and b) right side of the 17 *cm* long marked area. The length of a single picture amounts 10.6 *mm*.

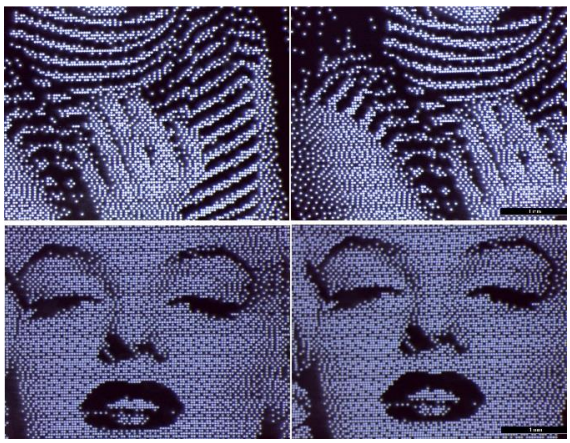

Fig. 15: Details of the marked pictures on the left and right side of the marked area.

## 3D structuring

First rectangles with the dimension 170 *mm* x 10.6 *mm* were machined in stainless steel 1.4301 with a marking speed of 25 *m*/*s*, a repetition rate of 2 *MHz*, an average power of 10 *W* at the wavelength 1064 *nm*. The pitch was chosen to be 12.5 $\mu m$ which is near the desired $w_0/2$. The random normal distribution of the starting points was realized by the two linear axes and the same bitmap was machined 30 and 100 times. With 30 repeats a surface roughness of $R_a = 0.3$ $\mu m$ was obtained. This

quite rough surface may be caused by the uncorrected pyramidal error which leads to a long-wave variation on the surface with deeper marks when the lines are closer. This effect becomes stronger with the number of repeats as illustrated in fig. 16.

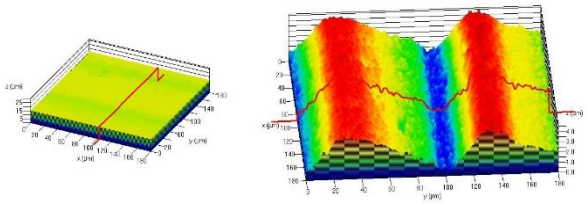

Fig. 16: Long-wave variation of the surface depth due to pyramidal error for 30 repeats (left) and 100 repeats (right).

Another effect can be observed at the right end of the rectangle where the border also shows periodic structures with a dimension of 90 $\mu m$ and a period of 100 $\mu m$ as shown in fig. 17. This period exactly equals the feed perpendicular to the marking direction within one turn of the polygon wheel. Therefore it is assumed that it is an effect of irregularities of the polygon wheel i.e. a combination of the pyramidal error leading to varying line distances and the position accuracy leading to varying spot positions with increasing distance to the starting position, especially for a marking speed of 25 *m*/*s* (see fig. 7).


Fig. 17: Right border of the machined rectangles with periodic structures of dimension 90 µm and a period of about 100 µm.

Squared pyramids with a base length of 1.2 *mm* served as model for real 3D structures. 105x5 pyramids with a distance of 1.6 mm between were machined into stainless steel with identical parameters as used for rectangles but with 204 slices. Microscope pictures of the single pyramids located at the beginning, 1/3, 2/3 and at the end of the marking area in scan direction are shown in Fig. 18 a). Again the pyramidal error can be observed as a periodic structure perpendicular to the marking direction. This structure becomes more pronounced with increasing distance to the start point of the marking lines which is in agreement with the observed periodic structures at the border of the machined rectangle (see fig. 17).

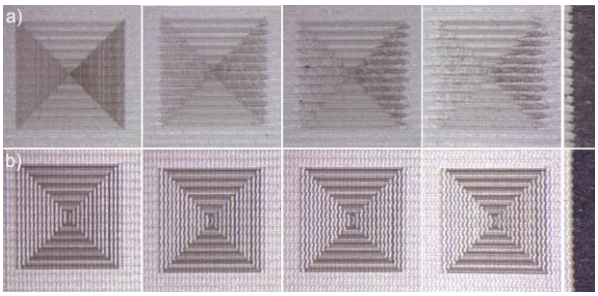


Fig. 18: Microscope images of single pyramids at the beginning, 1/3, 2/3 and end as well as the right border of the marking area (extension of 170x8 *mm*) The base length of a pyramid amounts 1.2 *mm*.
a) Marked with a marking speed of 25m/s and a repetition rate of 2 MHz resulting in a pitch of 12.5 µm.
b) Marked in "interlaced" mode with a marking speed of 100m/s and a repetition rate of 2 MHz resulting in an effective pitch of 12.5 µm.

The restriction in the marking speed is given by the limited maximum repetition rate of the laser PoD-module. Even the FUEGO system offers with 3 *MHz* the highest available one on the market, the marking speed would be limited to 37.5 m/s when a pitch of half of a spot radius should be conserved. But if the PoD gating module would allow the switching of pulses at 8 *MHz* a 3D structuring process with 100 *m*/*s* marking speed and at the highest average power of 43 *W*, representing the optimum point according to (3) for steel at this repetition rate, would be possible. An alternative to work at these high speeds at a low repetition rate of 3 *MHz* and less is offered by some kind of interlaced scanning. For this the bitmap is divided e.g. into four sub bitmaps containing column 1,5,9…., column 2,6,10…., column 3,7,11… and column 4,8,12…. . These bitmaps are then marked with 100 *m*/*s* marking speed and 2 *MHz* repetition rate. Between two sub bitmaps the starting point is shifted by 12.5 $\mu m$ with the second linear stage. Finally this should correspond to a marking procedure with 8 *MHz* and 100 *m*/*s* but in four steps. The corresponding results will help to estimate the machining quality which could be obtained when the PoD-module would allow switching of single pulses at 8 MHz. The corresponding result is shown in Fig. 18 b). The pyramidal error is still present but the smearing of the borders, increasing from left to right, is much less pronounced and the overall quality of the pyramids is significantly higher.

## Conclusion

Polygon scanners are very attractive beam deflecting devices if high marking speeds are demanded. Via the SuperSync$^{TM}$ technology the synchronization of the tested LSE170 with ultra short pulsed systems in MOPA arrangement becomes possible. The spot positions at the line start were always synchronized for all tested marking speeds, whereas they seem to lose the clock with increasing marking distance for low marking speeds, in contrast to common galvo scanners where problems are normally observed at high marking speeds. But at the high marking speeds of 70 *m/s* and 95 *m/s* the specifications of $\pm 5\ \mu m$ position accuracy and $\pm 3\ \mu m$ repeatability were even partially outnumbered which was demonstrated with the 2D structuring experiments. A loophole to use high marking speeds with improved accuracy and still conserving the pitch of half of a spot radius is offered by an "interlaced" scan strategy. This method has significantly improved the quality of the 3D structures.

But besides all these considerations the correction of the pyramidal error rests essential. It has to be done inside the polygon scanner device e.g. by adding an additional controllable fast mirror.

Finally one can conclude that the structuring strategies developed on the synchronized galvo scanner can successfully be transferred to the synchronized polygon scanner. But to obtain best possible results at high throughput and high speed some improvements on the PoD gating module of the laser system and the handling of the polygon errors have still to be done.

## Acknowledgement

This work was partially supported by the Swiss Commission for Technology and Innovation CTI

## References

[1] B. Jaeggi, B. Neuenschwander, U. Hunziker, J. Zuercher, T. Meier, M. Zimmermann, K.H. Selbmann and G. Hennig, "Ultra high precision surface structuring by synchronizing a galvo scanner with an ultra short pulsed laser system in MOPA arrangement", Proceedings of SPIE vol. 8243 (2012)

[2] B. Jaeggi, B. Neuenschwander, U. Hunziker, J. Zuercher, T. Meier, M. Zimmermann and G. Hennig, "High precision and high throughput surface structuring by synchronizing mechanical axes with an ultra short pulsed laser system in MOPA arrangement", ICALEO 2012, Paper M1207 (2012)

[3] B. Jaeggi, B. Neuenschwander, T.Meier, M. Zimmermann and G. Hennig, „High throughput laser micro machining on a rotating cylinder with ultra short pulses at highest precision", Proceedings of SPIE vol. 8607 (2013)

[4] S. Nolte, C. Momma, H. Jacobs, A. Tünnermann, B.N. Chichkov, B. Wellegehausen et al., "Ablation of metals by ultrashort laser pulses", J. Opt. Soc. Am. B / Vol 14, No. 10 / October 1997

[5] B.N. Chichkov, C. Momma, S. Nolte, F. von Alvensleben, A. Tünnermann, "Femtosecond, picosecond and nanosecond laser ablation of solids", Appl. Phys. A 63, 109-115 (1996)

[6] C. Momma, S. Nolte, B.N. Chichkov, F. v. 6lvenleben, A. Tünnermann, "Precise laser ablation with ultrashort pulses", Appl. Phys. Sci. 109/110, 15-19 (1997)

[7] G. Raciukaitis, M. Brikas, P. Gecys, B. Voisiat, M. Gedvilas, "Use of High Repetition Rate and High Power Lasers in Microfabrication: How to keep Efficiency High?", JLMN Journal of Laser Micro/Nanoengineering; Vol. 4 (3), p186-191 (2009)

[8] B. Neuenschwander, G. Bucher, C. Nussbaum, B. Joss, M. Muralt, U. Hunziker et al., "Processing of dielectric materials and metals with ps-laserpulses: results, strategies limitations and needs", Proceedings of SPIE vol. 7584, (2010)

[9] B. Neuenschwander, G. Bucher, G. Hennig, C. Nussbaum, B. Joss, M. Muralt, S. Zehnder et al., "Processing of dielectric materials and metals with ps laserpulses", ICALEO 2010, Paper M101 (2010)

[10] B. Neuenschwander, B. Jaeggi and M. Schmid, „from fs to sub-ns: Dependence of the material removal rate on the pulse duration for metals", Physics Proceedia, Vol. 41, pp. 787 – 794 (2013)

[11] B. Neuenschwander, B. Jaeggi, M. Schmid, "from ps to fs: Dependence of the material removal rate and the surface quality on the pulse durations for metals, semiconductors and oxides", ICALEO 2012, Paper M1004 (2012)

[12] F. Siegel, V. Schuetz, U. Stute, R. Kling, „Large-Scale Riblet Surfaces using Multi-Spot Micro Machining", ICALEO 2010, Paper M205, (2010)

[13] S. Bruening, G. Hennig, S. Eifel, A. Gillner, "Ultrafast Scan Techniques for 3D-µm Structuring of Metal Surfaces with high repetitive ps-laser pulses", Physics Proceedia, Vol. 12, pp. 105-115 (2011)

[14] K. Du, S. Brüning, A. Gillner, "High power picosecond laser with 400W average power for large scale applications", Proceedings of SPIE vol. 8244 (2012)

[15] R. De Loor, "Polygon scanner system for ultra short pulsed laser micro-machining applications", Physics Proceedia, Vol. 41, pp 537-544 (2013)

[16] http://www.ilt.fraunhofer.de/content/dam/ilt/en/documents/annual_reports/JB11/JB11_P51.pdf

[17] G.F. Marshall and G.E. Stutz, "Handbook of Optical and Laser Scanning", CRC Press, 2nd Ed., p. 256 (2012)

[18] B. Neuenschwander, B. Jaeggi, M. Schmid, A. Dommann, A. Neels, T. Bandi, G. Hennig, „Factors controlling the incubation in the application of ps laser pulses on copper and iron surfaces", Proc. of SPIE Vol. 8607 (2013)

[19] http://de.gdefon.com/